УДК 539.1.07

COSMIC TEST OF HONEYCOMB DRIFT CHAMBERS

A.A.Bel'kov, Yu.T.Kiryushin, A.A.Moshkin, S.A.Solunin, S.A.Vassiliev, A.V.Vishnevsky, D.A.Vishnevsky

The status of the test of pokalon-C honeycomb drift chambers by cosmic rays is presented. We discuss the cosmic track reconstruction, autocalibration of drift chambers and identification of cross-talk hits. Preliminary results of the test performed for drift chambers with 5 mm cells are given.

The investigation has been performed at the Laboratory of Particle Physics, JINR.

Испытания сотовых дрейфовых камер в космических лучах

А.А.Белъков и др.

Представлено состояние дел по испытанию в космических лучах сотовых дрейфовых камер, изготавливаемых из покалона-С. Обсуждаются такие методические вопросы, как восстановление треков космических частиц, автокалибровка дрейфовых камер и идентификация наведенных сигналов. Приведены предварительные результаты испытаний дрейфовых камер с размером ячеек 5 мм.

Работа выполнена в Лаборатории сверхвысоких энергий ОИЯИ.

1. Introduction

The Laboratory of Particle Physics of JINR, Dubna, is involved in the production of 5 mm honeycomb drift chambers made of pokalon-C foils for the PC superlayres of the Outer Tracker of the HERA-B detector [1]. The layer structure of the drift chamber modules is as follows.

- A 5 mm monolayer consists of 32 cells of hexagonal form. It is obtained by gluing two pokalon-C foils of semihexagonal form together. The distance between anode wires is 8.7 mm.
- After gluing an additional foil onto a monolayer, one obtains a single layer which is the smallest unit with 64 cells (wires) used in the Outer Tracker. Another two foils make a double layer.
- Modules of PC chambers produced at JINR are either single or double layers with 64 or 128 wires, respectively.

After manufacturing, all the modules are tested in cosmic rays to check their capability and measure their drift characteristics ($r(t)$ relation), spatial resolution as well as efficiency and cross-talk rate. The present note gives the status and preliminary results on the cosmic test of 5 mm honeycomb chambers at JINR.

2. Set-Up for Chamber Testing

The test rig for drift chambers testing in cosmic rays is shown schematically in Fig.1. It consists of the following main parts:

- a gas-tight box containing three modules (double layers) of honeycomb drift chambers with cell size of 5 mm which are being tested;
- two modules of monitor drift chambers, the first of them is placed above the tested chambers and the second one below;
- a transverse hodoscope consisting of two planes (upper and lower) of scintillation counters;
- upper and lower longitudinal scintillation counters to accomplish the trigger signal when cosmic particles are passing through the set-up.

The monitor drift chambers, between which the chambers under testing are placed, are honeycomb pokalon-C chambers with a cell size of 10 mm. Every chamber is a double layer with 64 cells (wires). Both upper and lower modules are placed in gas-tight boxes. The hits in the monitor chambers are used as the «basis» to reconstruct the tracks of penetrating particles in the chambers being tested.

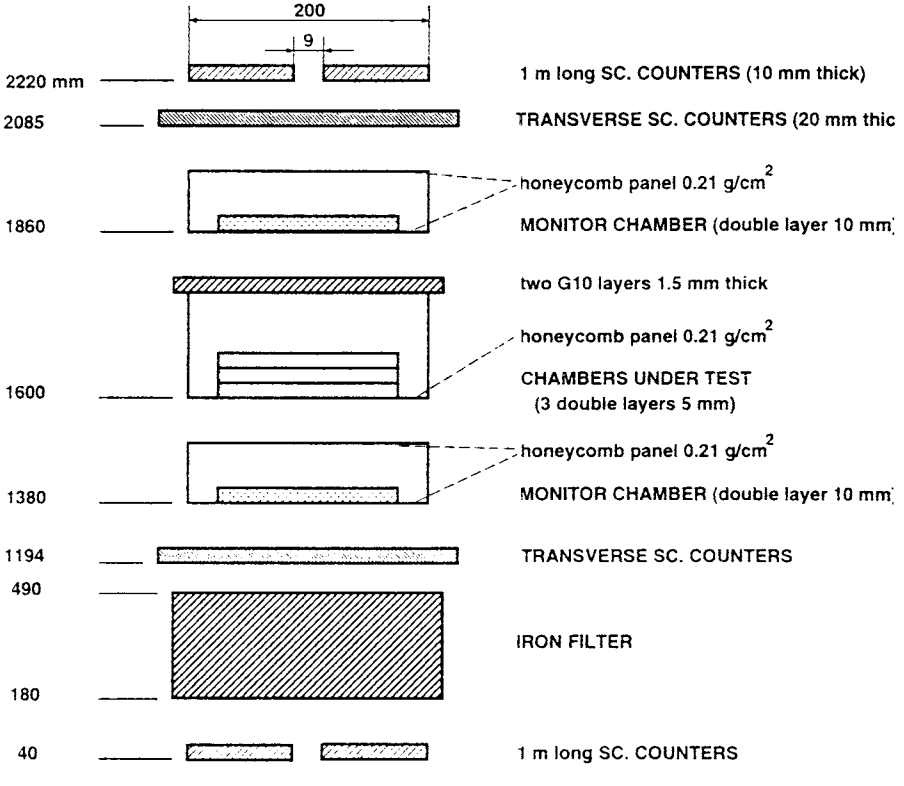

Fig.1. Schematic view of the stand for the cosmic test

The transverse hodoscope consists of two scintillation counter planes, each of which includes 6 counters. The transverse hodoscope gives additional information about the track position along the anode wires of the monitor and of the tested drift chambers. The honeycomb cells of the 55 mm modules contain various combinations of 25 μm thick sensitive wires and 75 μm thick insensitive wires which are connected with the sensitive wires to transport a signal. The counters overlap the sensitive and insensitive areas of the tested chambers along the wires in such a way that the signals from the transverse hodoscope could be used to resolve the combinatorics problems when measuring the cell efficiency of the 5 mm drift chambers.

The iron filter of 310 mm thickness is used to discriminate the low energy components of the cosmic radiation.

The trigger system is based on the scintillation counters. The upper and lower counter planes are tuned for coincidence. The upper plane counters have two photomultipliers on each plastic (one on each end). The signal from this plane is created if, at least, one photomultiplier has fired from each end. The lower plane counters have four photomultipliers on each plastic (two on each end). Every side of the counter is tuned for coincidence to provide a better background suppression. The signal from the lower plane is produced if, at least, one pair of the photomultipliers has fired on one of the counters from each end. The reference timing of the moment of the particle passing is determind by the lower plane. The precision of the timing point for every counter is about 1 ns.

The read-out system. The signals from the drift chamber are amplified using ASD-8 boards and are then fed through a converter into a TDC LeCroy-4291. The TDCs operate in Common Stop mode. Using the AUTOTRIM function, approximately the same delays and slopes of the count characteristics are set automatically for all TDCs. The trigger signal is connected to the ICL (Input Control Logic) which generates the Common Stop signal and the strobe for filling the input register as well as setting the LAM on the CAMAC bus. In case the information is not yet red out, the ICL blocks the writing into the TDC and the input register. A RESET is sent after read-out and then the ICL is ready for the next event. Pattern units are used for the transverse scintillation counters.

The electricity supply system provides the necessary voltages to the drift chamber and other parts of the stand. The working point is selected approximately at the end of the plateau of the dependence of the chamber efficiencies on the voltage for the given gas mixture.

The gas system provides a gas flow of about 10 l/hour.

3. Primary Calibration

At this step the dependence of the drift distance on the drift time ($r(t)$ relation) can be obtained as a first approximation of chamber calibration by integrating the corresponding drift time spectrum.

The following histograms are filled during the primary calibration of the drift chambers:

• **Wire occupancies** of every single layer for both the monitor chambers and the chambers under test. Typical wire occupancy histograms for the tested chambers are shown in Fig.2. They clearly show noisy and dead channels.

• **TDC count spectra** for all wires as two-dimensional histograms for every single layer and as sum spectra for all single layers. The value of one TDC count channel is equal to 1 ns.

• **Delay** T_0 for every wire is determined from the linear extrapolation to zero of the right hand slope of the TDC count spectrum for the wire.

• **Drift time spectra** for all wires are filled as a two-dimensional histogram for every single layer and as sum spectra for all single layers. The drift time is determined as difference $t = T_0 - T_{\mathrm{TDC}}$, where T_{TDC} is the TDC count.

Assuming that the drift cells are irradiated by the cosmic rays homogeneously, one can define the $r(t)$ relation by the integral

$$r(t) = \frac{r_{\max}}{N_{\mathrm{tot}}} \int_0^t \frac{dN}{dT} \cdot dT.$$

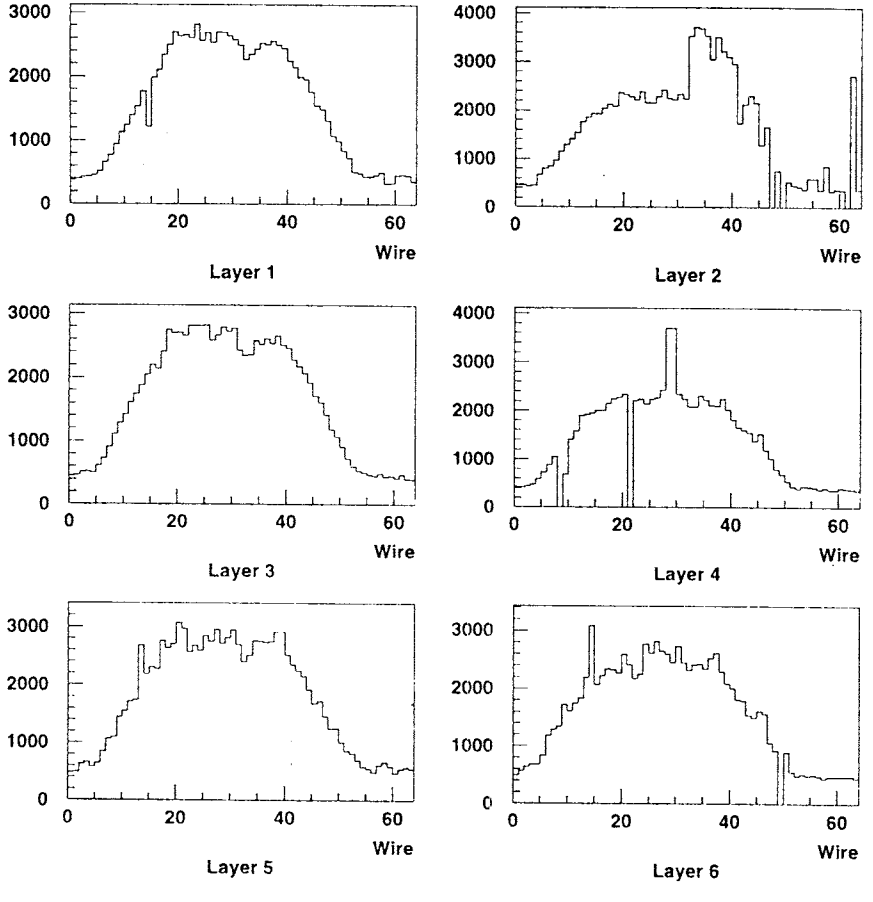

Fig.2. Wire occupancies for the 5 mm tested chambers. Single layers are enumerated from the bottom to the top for the 3 tested chambers inside the gas-tight box

Here r_{max} is the maximum drift distance in the chamber cell ($r_{max} = 2.9$ mm for 5 mm cells), N_{tot} is the total number of events in the histogram of the drift time spectrum, dN/dT is the drift time distribution.

4. Track Reconstruction and Cross-Talk Identification

To reconstruct a cosmic particle track in the drift chambers, only events having at most one cluster with at most four neighbouring hits in both the upper and lower monitor chambers (double layers), are used. In every single layer of the tested chambers the hits are grouped in clusters with at most three hits. Then only those clusters of hits in the tested chambers are selected whose «center-of-gravity» falls into a 8.7 mm wide corridor around the straight line passing through the «centers-of-gravity» of the clusters in the monitor chambers. All the selected hits, both in the monitor and tested chambers, are identified as belonging to the same trace of the cosmic particle.

For every event with L selected hits, the projection of the particle track onto the XY plane perpendicular to the wires is fitted with a straight line $x = ay + b$. The track parameters a and b are determined from the minimization of the χ^2 function:

$$\chi^2 = \frac{1}{L-2} \sum_{i=1}^{L} W_i^2 (D_i - S_i r_i)^2. \qquad (1)$$

Here the weights W_i are equal to the inverse of the estimated resolution, and

$$D_i = \frac{ay_i - x_i + b}{\sqrt{a^2 + 1}}$$

is the perpendicular distance between the track and the wire with coordinates (x_i, y_i), r_i is the measured drift distance given by the current $r(t)$ relation, $S_i = \pm 1$ is the parameter of the left/right ambiguity. Minimization of the function (1) is performed by the iterative method described in Ref.2.

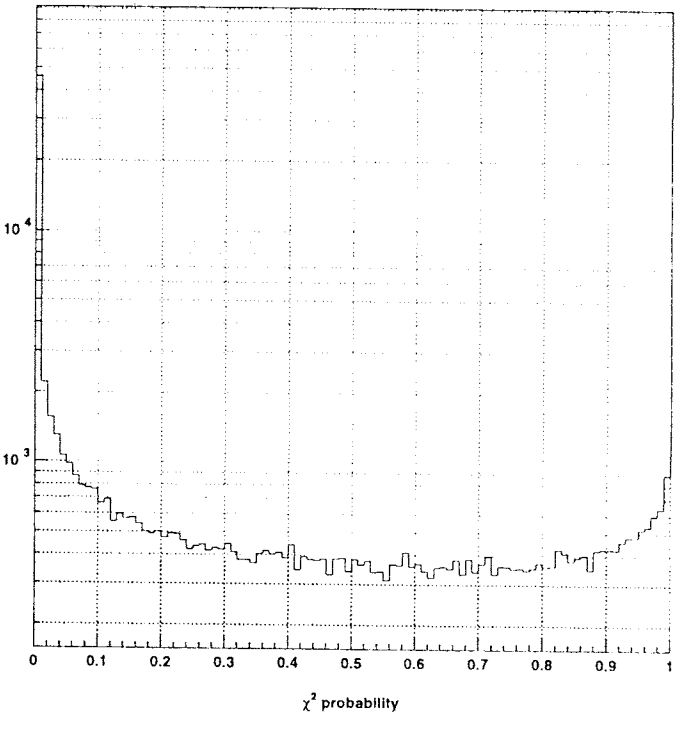

Fig.3. χ^2 probability for all tracks of particular run

The χ^2 probability is calculated for every event to estimate the quality of the track reconstruction. The distribution of the χ^2 probability for all tracks of a particular run is shown in Fig.3. For small probability values, there is a significant peak above the expected flat distribution. This peak indicates problems in the track reconstruction arising from noise and cross-talk hits and systematic uncertainties in the definition of the $r(t)$ relation. To perform the autocalibration of the drift chambers and measuring the cell efficiency, only tracks with χ^2 probability larger than 0.01 have been used.

To identify cross-talk hits in the 5 mm tested chambers, the same pattern recognition algorithm as described above can be used to provide the basic track in the tested chambers, stretched through the clusters in the monitor chambers. After selecting the clusters in the tested chambers, whose «centers of gravity» lie inside the corridor around the basic track, the difference $\Delta_i = |x_i - (ay_i + b)|$ is calculated for every i-th hit in the tested chambers. The hits for which $\Delta_i > r_{\max}$ are treated being cross talks or noise.

5. Autocalibration

The precision of the $r(t)$ relation can be improved by using an iterative autocalibration procedure to obtain a correction $\Delta(t)$ to the dependence $r(t)$, derived from the drift time spectrum in the primary calibration. The autocalibration correction $\Delta(t)$ is extracted from the straight line fit of the cosmic data by minimization of the total error function

$$F = \sum_{n=1}^{N} \frac{1}{L-2} \sum_{i=1}^{L} W_i^2 V_i^2. \tag{2}$$

Here the first sum is performed over all fitted tracks, while the second runs over all selected hits on the track,

$$V_i(a_n, b_n, \Delta) = \frac{a_n y_i - x_i + b_n}{\sqrt{a_n^2 + 1}} - S_i(r_i + \Delta(t_i)),$$

where a_n and b_n are the fitted parameters of n-th track.

Following [2], we perform a linearization of the error function (2), i.e., approximate the function F in such a way that all derivatives $\partial F/\partial a_n$, $\partial F/\partial b_n$ and $\partial F/\partial \Delta$ become linear on a_n, b_n and Δ. For this purpose the Taylor expansion of V_i around «the working point» $(\bar{a}_n, \bar{b}_n)$ is used:

$$V_i(a_n, b_n) = V_i(\bar{a}_n, \bar{b}_n) + (a_n - \bar{a}_n) \frac{\partial V_i}{\partial a_n}\Big|_{\bar{a}_n, \bar{b}_n} + (b_n - \bar{b}_n) \frac{\partial V_i}{\partial b_n}\Big|_{\bar{a}_n, \bar{b}_n} + \cdots$$

$$= \frac{\bar{a}_n y_i - x_i + \bar{b}_n}{\sqrt{\bar{a}_n^2 + 1}} - S_i(r_i + \Delta(t_i)) + \frac{a_n - \bar{a}_n}{(\bar{a}_n^2 + 1)^{3/2}} (y_i + \bar{a}_n x_i - \bar{a}_n \bar{b}_n)$$

$$+ \frac{b_n - \bar{b}_n}{\sqrt{\bar{a}_n^2 + 1}} + \cdots \approx A_i + E_n B_i + G_n - S_i \Delta(t_i),$$

where

$$A_i = \frac{\bar{a}_n y_i - x_i + \bar{b}_n}{\sqrt{\bar{a}_n^2 + 1}}, \quad B_i = y_i + \bar{a}_n x_i - \bar{a}_n \bar{b}_n,$$

$$E_n = \frac{1}{N_n^2 - P_n M_n} \sum_{i=1}^{L} W_i^2 S_i \Delta(t_i)(N_n - P_n B_i),$$

$$G_n = \frac{1}{N_n^2 - P_n M_n} \sum_{i=1}^{L} W_i^2 S_i \Delta(t_i)(N_n B_i - M_n)$$

with

$$M_n = \sum_{i=1}^{L} W_i^2 B_i^2, \quad N_n = \sum_{i=1}^{L} W_i^2 B_i, \quad P_n = \sum_{i=1}^{L} W_i^2.$$

In case of a polynomial parametrization of the autocalibration correction

$$\Delta(t) = \sum_{k=0} d_k t^k,$$

the error function (2) can be rewritten in the form:

$$F = \sum_{n=1}^{N} \frac{1}{L-2} \sum_{i=1}^{L} W_i^2 \left[A_i + \sum_{k=0} d_k (Q_n^{(k)} B_i + f_n^{(k)} - t_i^k S_i) \right]^2,$$

where

$$Q_n^{(k)} = \frac{1}{N_n^2 - P_n M_n} \sum_{i=1}^{L} W_i^2 S_i t_i^k (N_n - P_n B_i),$$

$$F_n^{(k)} = \frac{1}{N_n^2 - P_n M_n} \sum_{i=1}^{L} W_i^2 S_i t_i^k (N_n B_i - M_n).$$

Our consideration is limited to a cubic parametrization of the autocalibration correction. In this case the minimization conditions $\partial F / \partial d_k = 0$ ($k = 0, 1, 2, 3$) lead to a system of linear equations

$$\sum_{k=0} d_k \alpha_l^{(k)} = -\beta_l \quad (l = 0, 1, 2, 3),$$

where

$$\alpha_l^{(k)} = \sum_{n=1}^{L} \frac{1}{L-2} \sum_{i=1}^{L} W_i^2 (Q_n^{(k)} B_i + F_n^{(k)} - t_i^k S_i)(Q_n^{(l)} B_i + F_n^{(l)} - t_i^l S_i),$$

$$\beta_l = \sum_{n=1}^{L} \frac{1}{L-2} \sum_{i=1}^{L} W_i^2 A_i (Q_n^{(l)} B_i + F_n^{(l)} - t_i^l S_i).$$

6. Preliminary Results

To tune the hardware and the software for the cosmic test, a series of cosmic ray irradiations of the chambers was performed on the stand. The gas mixture Ar (30%) + + CO_2 (50%) + CF_4 (20%) was used. On the monitor chambers with the 10 mm cells, a high voltage of 2400 V was applied at an ASD threshold of 1.3 V. The tested chambers with the 5 mm cells were under a high voltage of 2100 V at a registration threshold of 0.9 V.

At a stage of primary calibration, as a result of integrating the drift time spectra for the monitor and tested chambers, initial $r(t)$ relations were obtained (see Fig.4, first iteration of the chamber calibration). The convergence of the iterative procedure of the chamber autocalibration described in section 4, is rather fast and the necessary precision can be reached after a few iterations. Figure 4 shows the $r(t)$ relations for the monitor and tested drift chambers after five iterations of the autocalibration procedure. Figure 4 also shows the residual distributions with RMSes corresponding to an average spatial resolution of 154 μm for the monitor 10 mm chambers and of 192 μm for the tested 5 mm chambers.

After performing the autocalibration procedure for both the monitor and tested chambers, the final $r(t)$ relations are used to repeat once again the cosmic-data analysis and to fill the following histograms:

• **Cell efficiency** for every wire of the monitor and drift chambers calculated as the ratio:

$$\varepsilon = N_{\text{found}} / N_{\text{expect}},$$

where N_{found} is the number of expected and found hits for a given cell, N_{expect} is the number of expected hits for the same cell.

• **Radial dependence of the cell efficiency** on the drift distance, averaged over all drift cells of every single layer in the monitor and tested chambers.

• **Residual** $\Delta r = r_{\text{mes}} - r_{\text{fit}}$ for all hits in every single layer of the monitor and tested chambers (r_{mes} is the measured drift distance for the hit, r_{fit} is the distance between the fitted track and the anode wire). The RMS of the residual distribution corresponds to the spatial resolution of the drift chamber with some correction factor.

The measured cell efficiencies are at the level of 92% for the monitor 10 mm chambers and of 97% for the 5 mm tested chambers. The dependences of the cell efficiencies on the drift distance for the monitor and tested chambers are shown in Fig.5.

For the tested 5 mm chambers, the selection of cross-talk and noise hits has been performed according to the algorithm described above. In this algorithm, the straight line passing through the clusters in the monitor chambers is used as a «basic» track for pattern recognition in the tested chambers. The cross-talk hits are at the level of about 15% of the total number of hits in the tested chambers. At the same time, the cross-talk hits are at the level of 45% for clusters with three hits and 16% for clusters with two hits. In case of single-hit clusters the cross-talk rate is not bigger than 1%.

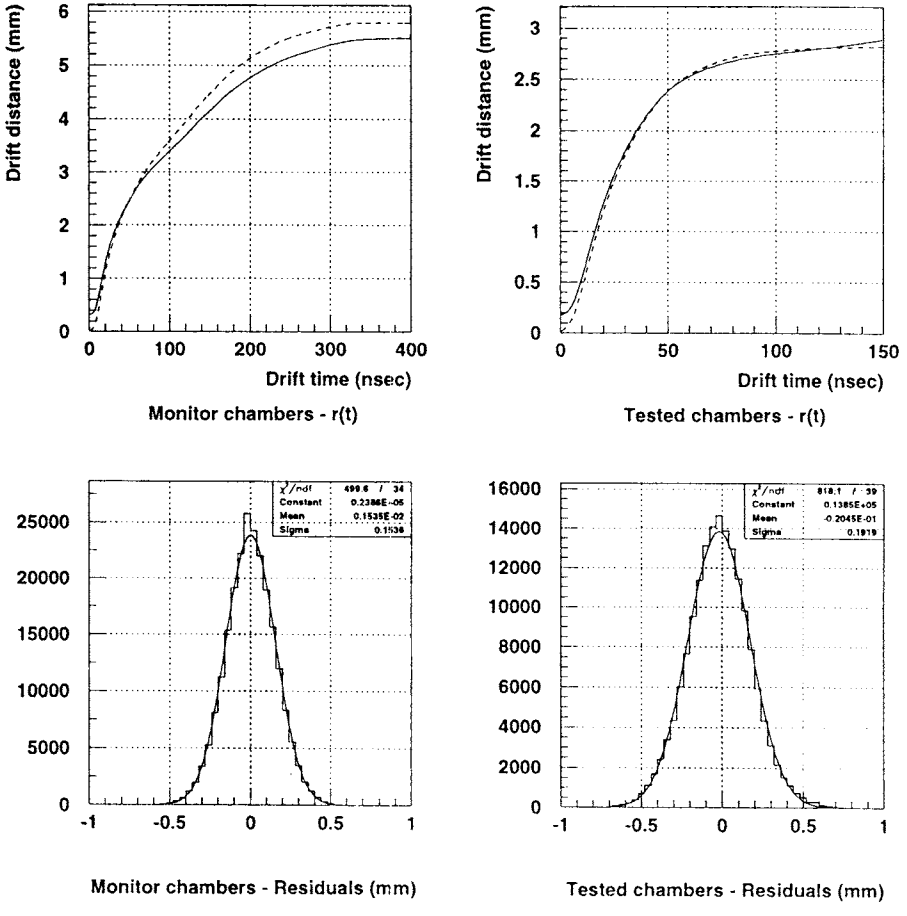

Fig.4. $r(t)$ relations and spatial resolutions for the monitor (left) and tested (right) drift chambers. The dashed lines in the upper pictures show the $r(t)$ relations obtained after the primary calibration. The solid lines correspond to the fifth iteration of the autocalibration procedure. The RMSes of the residual distributions in the lower pictures give an averaged spatial resolution of the chambers

7. Conclusion

This note gives a status report and preliminary results on the cosmic test of honeycomb drift chambers at JINR. Currently the set-up for the cosmic test is being upgraded. We have added one more scintillator counter, both into the upper and lower planes of the trigger system, and changed the TDCs with bad channels. The electronics of the read-out system should be modified properly to decrease the registration threshold to about 0.6 V. The aims of further studies with higher statistics are:

— further development of the autocalibration procedure with gas mixture and working point as relevant for HERA-B,

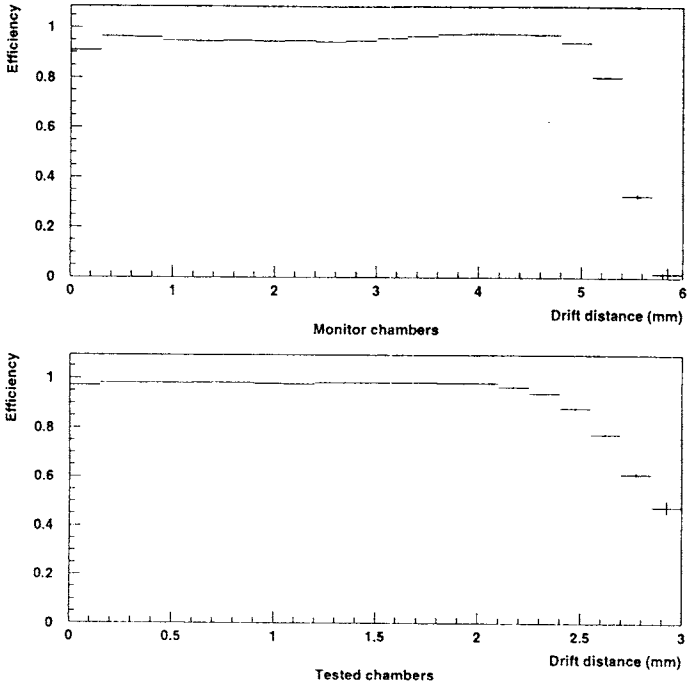

Fig.5. Dependences of the cell efficiency of the monitor and tested chambers on the drift distance

— improvement of the chamber resolution and study of its radial dependence,

— development of criteria for selecting noise and cross-talk hits.

This set-up can be used for testing any type of chambers. In this case the software would require only very small changes in the geometry.

We would like to thank U.Uwer and H.Kapitza for useful discussions and carefull reading of the manuscript.

References

1. Hartouni E. et al.— HERA-B collaboration, An Experiment to Study CP Violation in the B System Using the Internal Target at the HERA Proton Ring, Design Report, DESY-PRC 95/01, 1995.
2. Tolsma H.P.T. — The Honeycomb Strip Chamber: a Two Coordinate and High Precision Muon Detector, Universiteit Twente, PhD Thesis, 1996.

Received on June 8, 1998.